Large-Scale Lateral Entrainment and Detrainment at the Edge of a Geostrophic Shear Layer

MELVIN E. STERN*

Graduate School of Oceanography, University of Rhode Island, Narragansett, RI 02882

(Manuscript received 3 October 1986, in final form 3 March 1987)

ABSTRACT

The evolution of large-amplitude disturbances at the outer edge of a quasi-geostrophic shear layer depends on the sign of the outward gradient of potential vorticity. Entrainment of ambient water can occur when the gradient of relative vorticity dominates in the potential vorticity, and detrainment from the current can occur when the gradient of isopycnal thickness dominates. In the latter case long, thin filaments of finite area are "pinched off" into the surrounding water mass. This is verified using a quasi-geostrophic model having piecewise uniform potential vorticity. Contour dynamical calculations for many initial conditions allow us to define and tabulate an entrainment/detrainment velocity. This is used for an order of magnitude estimate of the flux of heat or salt on an isopycnal surface in a warm core ring.

1. Introduction

An early observation of lateral entrainment into the inshore edge of the Gulf Stream was obtained by Ford et al. (1952), who observed a long, thin and shallow filament of cold fresh shelf water embedded in the thermocline at very large distances downstream from its probable origin. More recent satellite and in situ observations of "shingles" have suggested (Stern, 1985) that wave breaking in the Gulf Stream region leads to the engulfment (entrainment) of shelf water, which is then strained by the stream to produce the thin structures necessary for small-scale mixing. The thin intrusive structures observed inside warm and cold core rings can be interpreted in a similar way (for references see the companion paper Stern, 1987).

An example of detrainment is provided by the familiar satellite pictures (Ramp, 1986) showing filaments of warm core rings being detached from the outer edge and mixed into the surrounding water mass.

In Stern's (1985) discussion of entrainment, a "1½-layer" density model with piecewise uniform potential vorticity was used. The undisturbed velocity profile of the lateral shear layer was such that the current vanishes on one side of an "interface" (a potential vorticity discontinuity) and has positive shear on the other side, so that the potential vorticity increases as the current increases. Such a shear layer is known to be stable to infinitesimal amplitude disturbances, and this situation is desirable in order to focus attention on large-amplitude disturbances (as will be specified in the initial state). When the downstream wavelength or scale of such disturbances is large compared to the Rossby radius of deformation, the weak initial downstream convergences amplify with time (see also Stern, 1986), thereby increasing the cross-stream velocities, steeping curves of constant potential vorticity (i.e., lateral "wave breaking" is produced), and engulfing ambient fluid into the shear layer. But the limited temporal duration of the calculation only suggested a subsequent pinching-off of a finite area of fluid. The effect is important because it may be the physical mechanism for initiating lateral diffusion and mixing. Further proof of the "pinching-off" is supplied herein by extending both the time interval and the parametric range of the previous calculation. A quantitative measure for the "entrainment velocity" will be defined and tabulated.

We will also show that the entrainment effect changes to "detrainment" when the sign of the potential vorticity gradient is reversed. This sign depends on the magnitude of the vorticity gradient relative to the gradient of isopycnal thickness. If the former is relatively large, as occurs at the inshore edge of parts of the Gulf Stream, then we have one sign. An example of the opposite sign occurs at the outer edge of round eddies, where the gradient of relative vorticity is usually smaller. In this case we shall show that the "parent" current can shed fluid into the surrounding water mass. Naturally both effects can occur over time so that no mass is transferred, but only properties like heat and salt.

Our conclusions for both cases will be based on a quasi-geostrophic model, and it must be clearly stated that the *quantitative* limits of validity of this asymptotic theory are exceeded when applied to the inshore edge of the Gulf Stream, and even to warm core eddies. But

* Present affiliation: Dept. of Oceanography, Florida State University, Tallahassee, FL 32306.

© 1987 American Meteorological Society

Unauthenticated | Downloaded 12/02/23 06:42 AM UTC

we believe that the basic cause of the entrainment/detrainment effects is qualitatively captured by our highly simplified model, and a liberal quantitative extrapolation may be permitted at this stage.

2. Formulation

For a two-layer ocean in which the lower layer is relatively deep and resting, the quasi-geostrophic potential vorticity of the upper layer is given by

$$\mathrm{PV} = \frac{g\Delta\rho}{\rho f^2}\left(\frac{\partial^2}{\partial x^2}+\frac{\partial^2}{\partial y^2}\right)\hat{h} - \hat{h}/H, \tag{1}$$

where H is its mean vertical thickness, $\hat{h}(x, y, t)$ is the deviation of the thickness from H, $\Delta\rho$ is the density deficit relative to the bottom layer of density ρ, f is the constant Coriolis parameter, and g is the acceleration of gravity. Note that a point PV vortex at (x', y') will induce a circularly symmetric streamfunction decreasing with distance as Bessel's function K_0, whereas a strictly barotropic system would have a logarithmic Green's function with a slower fall-off of velocity.

Consider Fig. 1a, the left-hand side of which depicts a *smooth* undisturbed shear layer $\bar{U}(y)$ having a relatively strong maximum cyclonic shear, so that the relative vorticity term in (1) dominates. The undisturbed potential vorticity $\overline{\mathrm{PV}}(y)$ therefore decreases as one goes from the stream into the resting fluid, and the minimum $\overline{\mathrm{PV}}$ gradient is at $y = y^*$. Of course the sign of this gradient would reverse at $y \ll y^*$ if there were a full *jet,* but we shall restrict our attention to a stable *shear layer* in order to avoid the infinitesimal amplitude instability which occurs for the jet, and in order to isolate our effect.

We then perturb the laminar flow with a finite amplitude initial ($t = 0$) disturbance, such that all the PV = constant curves are displaced towards positive y as indicated in Fig. 1a. This results in positive "potential vorticity anomaly":

$$\mathrm{PV}'(x, y, t) = \mathrm{PV}(x, y, t) - \overline{\mathrm{PV}}(y), \tag{2}$$

where $\overline{\mathrm{PV}}(y)$ is the value of (1) when $\hat{h} = \bar{h}(y)$, $\bar{U}(y) = -g(\Delta\rho/\rho)f^{-1}\partial\bar{h}/\partial y$. Then $h'(x, y, t) = \hat{h} - \bar{H}$ may be computed from

$$g(\Delta\rho/\rho)f^{-2}\nabla^2 h' - h'/H = \mathrm{PV}', \tag{2a}$$

and the total geostrophic velocity $\mathbf{V} = (u, v)$ may then be computed by adding $\bar{U}(y)$ to $g(\Delta\rho/\rho)f^{-1}\mathbf{k} \times \nabla h'$ where $\mathbf{k}$ is the unit vertical vector. The sense of the circular arrow in Fig. 1a indicates that all the initial PV′ anomalies are positive. Thus in each area element $(dx'dy')$ there is a positive elementary vortex tending

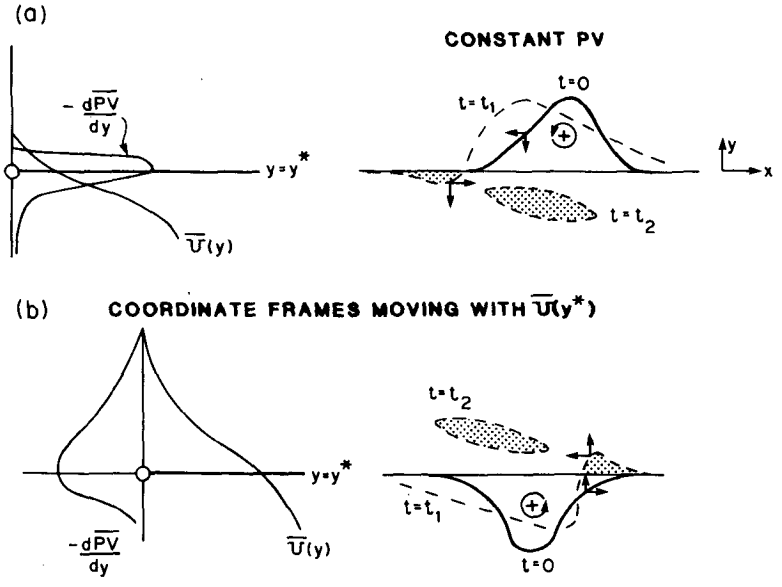

FIG. 1. The temporal evolution of finite amplitude initial perturbations of potential vorticity (PV) associated with the *smooth* undisturbed shear flow $\bar{U}(y)$ shown in the left panels. The extremum PV *gradient* curve ($y = y^*$) is drawn with a heavy line. (a) PV decreasing with y. The curve labeled $t = 0$ in the right-hand panel indicates the initial displacement of the PV curves, and the PV anomalies relative to $\bar{U}(y)$ are positive as indicated by the circular arrow. The straight arrows indicate the velocities induced by these anomalies. In our moving coordinate system, the constant PV curve evolves into the one labeled $t = t_1$, and at $t = t_2$ a pinched-off (entrained) eddy is formed as indicated by the stippled area. (b) As in (a) except PV increases with y and detrainment occurs.

Unauthenticated | Downloaded 12/02/23 06:42 AM UTC

to produce a counterclockwise and circular symmetric motion at any exterior point (x, y). By summing the contribution of the PV′ anomalies due to all the $dx'dy'$, and by adding $\bar{U}(y)$, we obtain $V(x, y)$. The small straight arrows indicate the net velocities at a point on the left-hand side of the $t = 0$ interface (Fig. 1a). This point moves leftwards [in a coordinate system moving with $\bar{U}(y^*)$] because $\bar{U}(y)$ decreases with y, and because the contribution of PV′ is in the same direction. For a large initial displacement the PV isopleth will therefore steepen on the left side, as indicated by the $t = t_1$ curve, and it is also displaced below $y = y^*$ because the induced y velocities (v) are negative in the region of the incipient trough. As the PV isopleth steepens, it tends to reinforce these negative v velocities by bringing more of the PV anomalies closer to the incipient trough. Moreover the relative $\bar{U}$ is positive in the trough (as indicated by the arrow), thereby causing further steepening of the isopleth between the trough and the ridge. The positive feedback effect causes this isopleth to become a multivalued function of x (wave breaking), and may even lead to a multiconnected state in which an entrained eddy "pinches off" as shown by the stippled area ($t = t_2$). If this is used as a tracer, then the continued downstream straining of the entrained lense will lead to large gradients of the tracer, which we associate with processes conducive to the formation of (T–S) fine structure and the eventual thermodynamic mixing of the lense.

The dynamical consistency of the foregoing idea will be verified using numerical solutions of the "contour dynamical" equations for a piecewise uniform potential vorticity model (Stern, 1985). In this model the continuous distribution of PV (Fig. 1a) is replaced by a discontinuity surface on either side of which PV is constant. The magnitude of the jump might be taken equal to the area of the $-\partial\overline{PV}/\partial y$ curve in the continuous models in Fig. 1, and the undisturbed values of $\bar{U}(y^*)$ in the two cases may be taken to be the same.

Figure 1b leads us to expect quite a different effect if the sign of undisturbed potential vorticity gradient is reversed. The changed sign occurs if the relevant y-scale of the shear layer is larger than the radius of deformation, so that the $\overline{PV}(y)$ distribution is determined mainly by $\bar{h}$ rather than $\partial\bar{U}/\partial y$. The $y = y^*$ level (the origin in Fig. 1b) is now taken at the maximum $\partial\overline{PV}/\partial y$, and the coordinate system again moves with $\bar{U}(y^*)$. If at $t = 0$ all PV isopleths are displaced towards $y = -\infty$ (as shown in Fig. 1b), then all the PV anomalies are positive, as indicated by the curved arrow, and the induced velocities are indicated by the straight arrows. These velocities and $\bar{U}(y)$ cause the right-hand face of the PV isopleth to steepen at $t = t_1$, and a ridge (stippled) is also induced. Under certain conditions to be discussed, the trough behind the steep front of the isopleth does not propagate downstream faster than the leading ridge, but it moves towards $y = y^*$ and thereby pinches off ($t = t_2$) the ridge. Quite a different evolution is expected if the sign of the initial displacements of the PV isopleths is reversed, because the anticyclonic anomalies would induce *positive* v on the left side of the isopleth and no trough (as in Fig. 1a) would be produced. Furthermore the right-hand side would not steepen because the shear of $\bar{U}(y)$ is in the wrong sense. Thus the entrainment/detrainment effect depends on the sign of these "single-lobed" initial disturbances. We shall also calculate the evolution of "two-lobed disturbances", and this will enable us to infer the qualitative behavior of more general initial configurations.

The piecewise uniform potential vorticity model has certain disadvantages as well as advantages over conventional (pseudospectral) two-dimensional (x, y) integrations of the quasi-geostrophic partial differential equations. The former method constrains us to unrealistically "bumpy" velocity profiles compared to the nice smooth ones that can be used with the latter method. However, the former method makes it easy to resolve the highly filamented structure which evolves from the larger scale and to develop a physical understanding. Furthermore, no artificial eddy viscosity is introduced in our calculation, and a wide range of initial configurations can be rapidly covered (all those reported here were done on a personal computer). The limitations of the piecewise uniform potential vorticity model can be explored by making reasonably analogous calculations in a *high*-resolution pseudo-spectral model.

The numerical technique and program used here are almost identical to the one in Stern (1985). We now include a finite shear above ($y < y^*$) the interface, whose effect is particularly important for detrainment (Fig. 1). It should be pointed out, however, that a complete pinch-off (Fig. 1) of an eddy will not occur in our nondiffusive model, but the "neck" of the eddy only gets thinner as $t \to \infty$. Since nature undoubtedly administers the *coup de grace* via small-scale turbulence, we shall take the liberty of performing neck "surgery" at a time when it is sufficiently thin. The area and the time at which this *virtual* "pinch-off" occurs are recorded, and from these numbers an entrainment/detrainment velocity is computed.

Our potential vorticity model gives results similar to those in barotropic models (Pullin, 1981), insofar as these also exhibit wave breaking and engulfment at early times. But at later times Pullin's calculation indicates that this fluid is "pushed back" into its original domain, rather than being pinched-off and entrained into the shear flow. But in our PV model we shall quite convincingly show that a *finite* area is pinched-off, and the reason will be attributed to the shorter range of the K_0 vortices.

3. Results

The $\hat{h}$ response to an elementary point potential vortex, as given by the Green's function for the differ-

Unauthenticated | Downloaded 12/02/23 06:42 AM UTC

ential operator (1), is the Bessel function K_0. Therefore if (1) is uniform above a known curve $y = L(x, t)$ and also uniform for $y < L(x, t)$, then we can compute the sum of the responses. From $\hat{h}$ we compute the geostrophic velocities on $L(x, t)$, and then the position of Lagrangian particles at $t + dt$. This gives $L(x, t + dt)$, and so on (Stern, 1985).

We make the results nondimensional by using the Rossby radius of deformation as the horizontal length scale, and by using H as the scale for the nondimensional layer thickness. Thus $\nabla^2 h - h$ is the nondimensional potential vorticity, and the jump in this across the nondimensional $L(x, t)$ is taken as ± 1. This implies that the unit for vorticity and the unit for $(\text{time})^{-1}$ is the jump across the interface, with the "+" sign corresponding to Fig. 1b and the "−" sign to Fig. 1a. The unit of horizontal velocity equals the ratio of the radius of deformation to the time scale. The $y = 0$ axis in that which follows corresponds to y^* in Fig. 1, and we also introduce the important nondimensional parameter

$$\Gamma = \frac{\text{undisturbed velocity on } y = y^*}{\text{velocity scale defined above}}. \tag{3}$$

The undisturbed nondimensional velocity profile is then given by

$$\bar{u}(y) = \begin{cases} \Gamma e^{-y}, & y > 0 \quad (4a) \\ \Gamma \cosh y - (\Gamma \pm 1) \sinh y, & y < 0, \quad (4b) \end{cases}$$

where "+" is to be used for PV decreasing with y and "−" is to be used for PV increasing with y. This shear layer is meant to represent the outer edge of a current, at which *localized* disturbances evolve. If these do not extend to large negative y then the large $\bar{u}(y)$ values in our model will not be significant. We require that $\bar{u}(y)$ decreases monotonically as y decreases, and therefore we stipulate that $\Gamma \leqslant 1$ when the "−" sign is used in (4b).

Numerical integration of the contour dynamical equations was made for a one-lobed disturbance,

$$L(x, 0) = A_1 \exp[-(x/W_1)^2], \tag{5}$$

having nonzero area above the y axis, and for a two-lobed disturbance,

$$L(x, 0) = \frac{2A_2(x/W_2)}{[1 + (x/W_2)^2]^2}, \tag{6}$$

having zero area.

When the scale width (W_1 or W_2) is much larger than unity and when the amplitude (A_1 or A_2) is of order unity, then $L(x, t)$ obeys a first-order hyperbolic partial differential equation [see Eq. (4.8) in Stern (1985)] which implies that the slope of L steepens continuously in time in those regions where $\partial L/\partial x > 0$. This result (obtained for PV decreasing with y) is easily generalized to the case where PV increases with y, and when this is done, we obtain a nonlinear propagation speed

$$C(L) = (\Gamma - 1/2)e^{-L}$$

$$(\Gamma > 1, \text{PV increasing with } y) \tag{7}$$

for each L in the initial state. Since this decreases with increasing L, it follows that for either Fig. 1a or 1b, the long-wave disturbances will tend to steepen in the region where L increases with x. It therefore suffices to consider the later evolutionary stage, by starting the numerical calculation with initial $L(x, 0)$ having order *unity* scales in the x direction.

The contour dynamical calculation for Fig. 2 confirms the expected (Fig. 1a) evolution for a single-lobed disturbance when PV decreases with y. Thus we see the left-hand side of $L(x, 0)$ steepening and breaking at $t = 2$. The transverse velocities $v < 0$ induced by the cyclonic anomalies form the trough ($L < 0$), which is then ($t = 8$) strained by the undisturbed shear below $y = 0$. The (short range) negative v on the left-hand side of maximum L cause the latter to move towards the x axis and to converge on the branch of the interface lying below $y = 0$ ($t = 12$). The merging branches cause a lense of low potential vorticity fluid to be surrounded

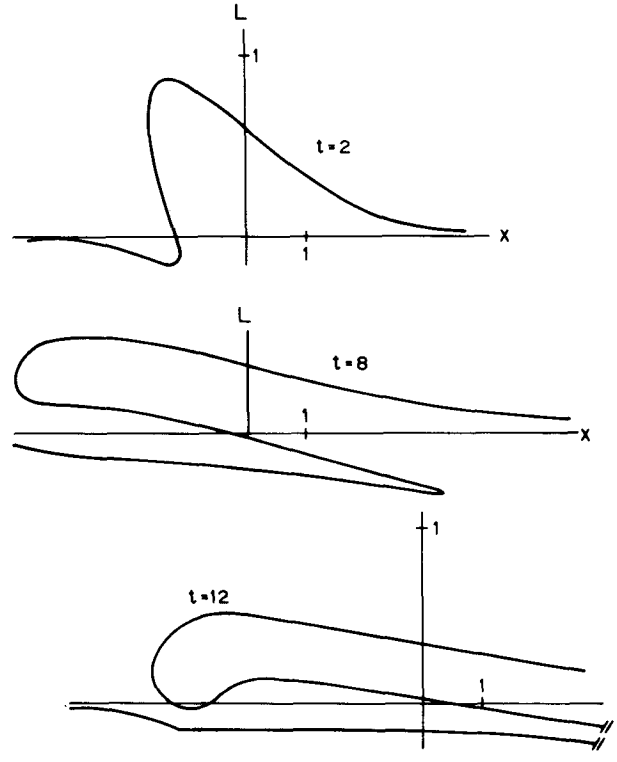

FIG. 2. Evolution of the interface in a coordinate system translating with speed $\bar{u}(0) = \Gamma$. PV decreasing with y, run 4A single lobe. Initial condition $A_1 = 1$, $W_1 = 1$, $\Gamma = 1$, time step $T = 0.1$, initial number of points $N = 103$. At $t = 8$ the distribution of data points was adjusted by adding some in sparse regions and deleting some in dense regions. The result of this at $t = 10$ was in excellent agreement with the result from the unaltered run at the same time. At $t = 17$ (not shown) a pinched-off entrained eddy occurs as the blunt nose ($t = 12$) approaches the other branch of the $L(x, t)$ curve.

Unauthenticated | Downloaded 12/02/23 06:42 AM UTC

by high potential vorticity fluid. Within the limits of our resolution, the "pinch-off" is essentially completed at $t = 17$ (not shown), and the area of the entrained fluid at that time is 1.63. From these two numbers a nondimensional entrainment velocity

$$u_e = \frac{(\text{entrained area})^{1/2}}{\text{interval of time from } t=0} \tag{8}$$

is computed to have the value $u_e = 0.075$. Decreasing the initial amplitude (A_1) by half (run 5A in Table 1) reduces the entrained area by a factor of five, but the pinch-off time is smaller because the $L > 0$ lobe has a shorter y-distance to go before coming into contact with the other branch ($y < 0$) of the interface. The effect of reducing Γ may be seen by referring to Fig. 11 of Stern (1985) for which $\Gamma = 0$, $W_1 = 1$, $A_1 = 1$.

Since an upstream trough is immediately generated by the single-lobed ridge, it is instructive to look at the evolution of a double-lobed initial disturbance (6) with $A_2 > 0$. Since this sign immediately puts a trough with anticyclonic vortices upstream of a ridge with cyclonic anomalies, we expect a reinforcement of the negative velocities at $x = 0$, and a more rapid pinching off than in Fig. 2. Figure 3 illustrates the effect for $1 = \Gamma = A_2 = W_2$, and at $t = 12$ (dashed curve only partially shown) there is a pinch-off of a thin lense of low PV fluid. An important factor (as previously mentioned) in the pinch-off process is the relatively short range inductive effect of the K_0 vortices as compared to barotropic vortices. In the latter case the velocities decay as $1/r$ whereas the decay is e^{-r} for PV vortices, where r measures radial distance. The effect of the more rapid decay appears in the behavior of the "nose" of the $L > 0$ lobe (i.e., the point with a minimum x) from $t = 9$ to $t = 12$ in Fig. 3. The positive vortices in this lobe cause the nose to move towards $y = 0$ and to converge on the other branch ($L < 0$) of the interface, which is less displaced because the induced velocities are smaller.

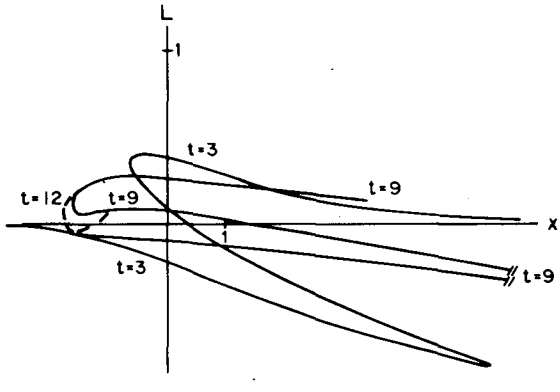

FIG. 3. PV decreasing with y; run 1A double lobed. $A_2 = 1$, $W_2 = 1$, $N = 103$, $\Gamma = 0.1$. At $t = 12$ only the nose is shown (dashed curve) since the rest of $L(x, 12)$ in the vicinity of pinch-off is virtually the same as the lower branch of the $t = 9$ curve.

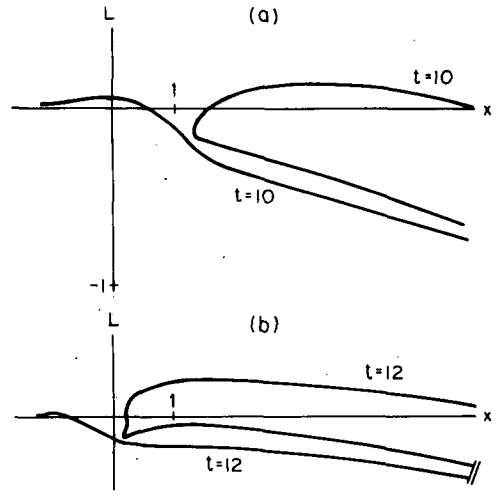

FIG. 4. As in Fig. 3 except with two different Γ. (a) Run 2A with $\Gamma = 0$, $A_2 = 1$, $W_2 = 1$. Pinch-off at $t = 12$ (not shown). (b) $\Gamma = 0.5$.

In a barotropic version of this problem, the convergence of the two branches would be less.

Figure 4a is a repeat of Fig. 6 in Stern (1985), except for a longer time interval and using more Lagrangian points. A (virtual) pinch-off occurs for this case ($\Gamma = 0$), and also for the intermediate value of $\Gamma = 0.5$ in Fig. 4b. The mathematically delicate question of whether or not a "true" pinch-off (i.e., a multiply connected domain) occurs need not detain us, and we are content with using a criterion such that the width of the neck of the pinch is considerably smaller than the maximum (y) width of the entrained lense. This crude criterion gives an O(10%) uncertainty in determining (8). Also note that this time is measured from some "initial" instant ($t = 0$) whose physical significance remains to be discussed (see §4).

Next we change the sign of the gradient of PV, and Fig. 5 verifies the detrainment effect expected (Fig. 1b) for a single-lobed disturbance with $L < 0$. Note that the pinch-off at $t = 12$ depends on the fact that the nose of the negative L lobe (i.e., the point with a maximum x) is not excessively strained by the shear below $y = 0$. Figure 5 shows that this max(x) is relatively stationary (in the moving coordinate system), so that the induced v velocities cause the ($L < 0$) nose to converge on the other branch ($y > 0$) of the interface. In this respect the pinch-off of a detrained eddy is similar to that (Fig. 2) for an entrained eddy. Figure 6 shows the striking difference which occurs when the sign of $L(x, 0)$ is reversed—the pinched-off streamer will have zero area. Table 1 lists the "detrainment velocity," this being defined in the same way as (8).

One may object to the foregoing calculation on the grounds that $\Gamma = 1$ yields an unrealistic $\bar{u}(y)$ having zero shear immediately below $y = 0$. Calculations have therefore been done with $\Gamma = 2$, which increases this shear to half the value above $y = 0$, thereby giving a

Unauthenticated | Downloaded 12/02/23 06:42 AM UTC

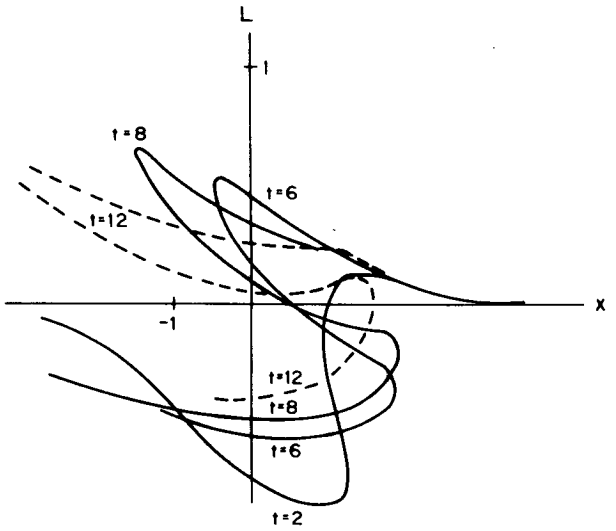

FIG. 5. PV increasing with y; single lobe initial condition. Run 2B: $\Gamma = 1$, $A_1 = -1$, $W_1 = 1$. A detrained eddy (dashed curve) is pinched off at $t = 12$. The (x, L) coordinates of the Lagrangian particle which is at the blunt nose at $t = 8$ are: $(-0.70, -0.61)$, $(0.33, -0.80)$, $(1.3, -0.66)$, $(1.75, -0.44)$, $(1.84, -0.22)$, $(1.6, -0.02)$, $(1.0, 0.07)$ at $t = 0, 2, 4, 6, 8, 10, 12$ respectively.

TABLE 1. Entrainment/detrainment characteristics.

Run/Fig. no.	Γ	A	W	Entrained area	Pinch-off time	u_e
		Decreasing potential vorticity with y				
1A/3	1	$A_2 = 1$	$W_2 = 1$	1.82	12	0.11
2A/4a	0	$A_2 = 1$	$W_2 = 1$	0.76	12	0.073
3A/4b	0.5	$A_2 = 1$	$W_2 = 1$	1.20	12	0.091
4a/2	1	$A_1 = 1$	$W_1 = 1$	1.63	17	0.075
5A/—	1	$A_1 = 0.5$	$W_1 = 1$	0.37	10	0.061
		Increasing potential vorticity with y				
				Detrained area		
2B/5	1	$A_1 = -1$	$W_1 = 1$	0.74	12	0.072
3B/10	1	$A_2 = 1$	$W_2 = 1$	0.72	12	0.070
7/7	2	$A_1 = -0.5$	$W_1 = 2$	0.37	14	0.043
2-2A/8	2	$A_2 = 1/3$	$W_2 = 1$	0.15	8	0.048
3C/9	2	$A_2 = 0.15$	$W_2 = 1$	4.4×10^{-3}	8	0.008
1C/	2	$A_2 = 1$	$W_2 = 1$	similar to run 4C, see text		
1B/6	1	$A_1 = 1$	$W_1 = 1$	0		
4C/11	2	$A_1 = 1$	$W_1 = 2$	no pinch-off, but engulfment		

more satisfactory representation of the smooth profile envisioned in Fig. 4b, in which the shear is relatively small below $y = y^*$. The result for Fig. 7 implies that the detrainment effect is not an artifact of the shear discontinuity (which is the price to be paid for using a simple piecewise uniform potential vorticity model).

Figure 8 shows the detrainment of a pinched-off eddy at $t = 8$ for a two-lobed disturbance of moderate amplitude (Table 1). If the initial amplitude is halved (Fig. 9) then run 3C in Table 1 shows that the detrained area is decreased by a factor of 30. When the amplitude is increased to $A_2 = 1$ (Fig. 10), we essentially have a pinch-off at $t = 12$ and the detrained area is increased. The detrainment coefficient u_d computed by a formula analogous to (7) does not change (Table 1) too much if $A > \frac{1}{3}$, and for this range the typical value

$$u_d \sim 0.05 \tag{9}$$

will be used in a subsequent order of magnitude calculation.

In Fig. 11 the shear and disturbance amplitudes are so large that the trough is advected rapidly downstream and a sharp nose forms, whereas in Figs. 5 and 7 a blunt and stationary nose forms because either the shear or disturbance amplitude is smaller. The large straining of the $L < 0$ nose (Fig. 11) leads to small v, which does not enable this nose to approach the $L > 0$ branch. Thus no pinch-off occurs, but only a thin filament of the current (stippled) is left behind as the surrounding water mass is engulfed.

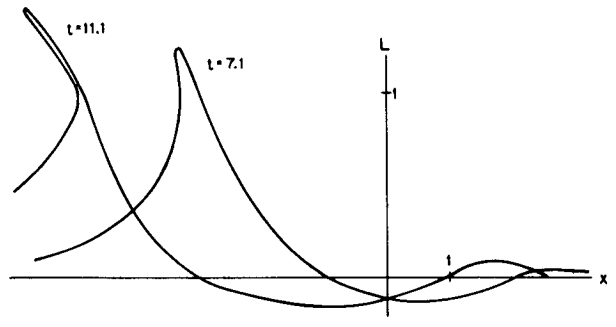

FIG. 6. Run 1B: As in Fig. 5 except $A_1 = +1$. The breaking wave at $t = 7.1$ gives rise to a streamer which pinches off shortly after $t = 11.1$ with zero area.

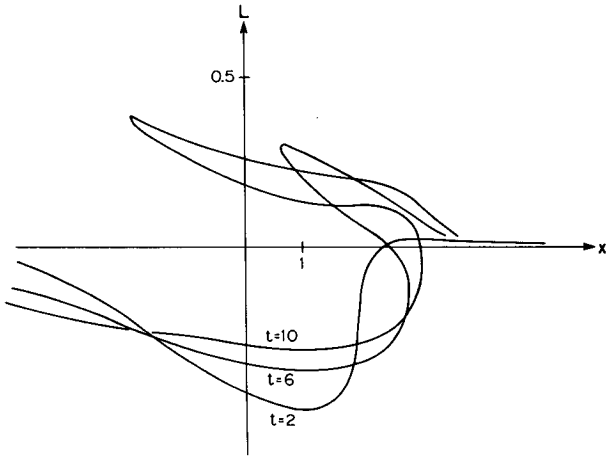

FIG. 7. PV increasing with y; single lobe. Run 7: $\Gamma = 2$, $A_1 = -\frac{1}{2}$, $W_1 = 2$, $N = 114$. At $t = 14$ (not shown) the width of the neck of the pinching-off eddy is half the value at $t = 10$.

Unauthenticated | Downloaded 12/02/23 06:42 AM UTC

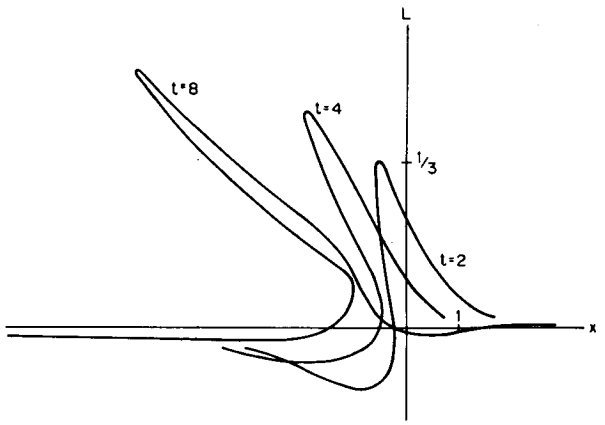

FIG. 8. PV increasing with y; double lobe. Run 2/2A: $\Gamma = 2$, $A_2 = \frac{1}{3}$, $W_2 = 1$, $N = 115$. At $t = 8$ a detrained eddy forms.

4. Conclusions

Slow downstream current variations of finite amplitude at the outer edge of a stable system evolve by steepening of the potential vorticity isopleths and by transferring energy to the cross-stream velocity. The subsequent lateral wave breaking can lead to entrainment of ambient fluid or detrainment, depending upon the direction of the potential vorticity gradient relative to the vorticity gradient. The short-range action of a potential vortex is responsible for the pinching off of a substantial fluid area in the post wave-breaking phase. An entrainment velocity has been computed from this area and from the time of its virtual pinch-off.

This theory should be regarded as a first attempt at quantifying lateral diffusion in a way that is both physically sound and consistent with structures observed at the subgeostrophic scale. To illustrate the applicability of the theory let us consider the isopycnal transport of heat and salt from a warm core ring to the far-field, focusing exclusively on the detrainment mechanism which is suggested by surface images of streamers extending outwards from the perimeter of the ring. We shall assume that at any random time (designated t = 0) there exists *one* finite amplitude disturbance on the perimeter evolving towards detrainment as described in this paper. This initial disturbance may have been introduced by other eddies (see Stern, 1987) or currents in the ambient fluid, or by the β effect, or by topography. We assume that after the first disturbance detrains, another finite disturbance springs up fairly rapidly and then evolves towards detrainment, etc. We assume that the characteristic cross-stream width of the disturbance is of the order of the radius of defor-

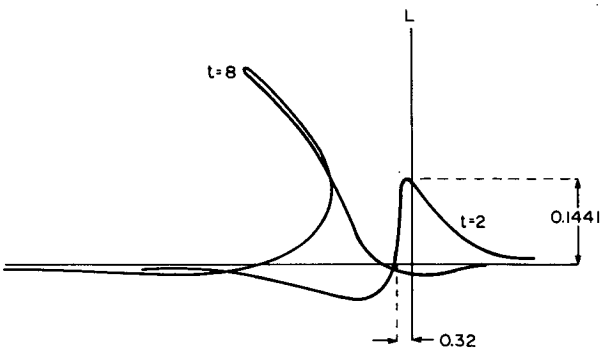

FIG. 9. Run 3C: As in Fig. 8 except $A_2 = 0.15$.

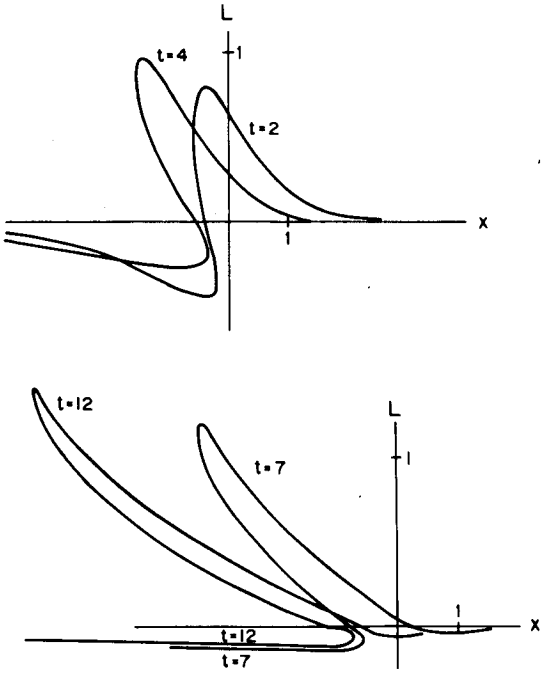

FIG. 10. PV increasing with y. Run 3B: Double-lobed. $\Gamma = 1$, $A_2 = 1$, $W_2 = 1$. As in Fig. 9 except larger amplitude.

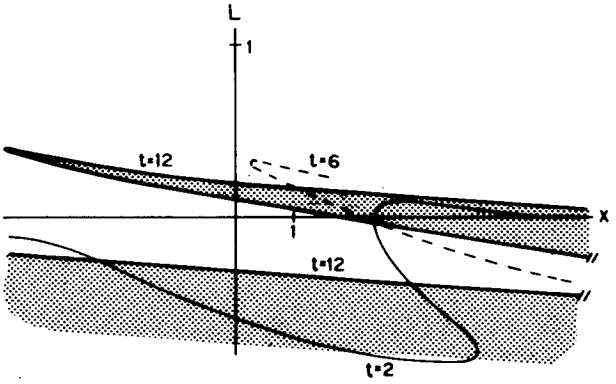

FIG. 11. Run 4C: Single lobe. $\Gamma = 2$, $W_1 = 2$, $A_1 = 1$, PV increasing with y. This run is the same as in Fig. 7 except that the disturbance amplitude is doubled, and it is essentially the same as in Fig. 5 except the shear below $y = y^*$ is larger. No detached eddy forms in this case, but the slow high PV fluid is engulfed by the low PV fluid (stippled).

Unauthenticated | Downloaded 12/02/23 06:42 AM UTC

mation l, and $U = \bar{U}(y^*)$ is the characteristic velocity which determines the characteristic vorticity variation and the time scale l/U in our model. The nondimensional detrainment velocity is then

$$u_d = \frac{(\text{change in area}/l^2)^{1/2}}{(\text{change in time})(U/l)}. \tag{10}$$

Let Δt denote the time that it would take for the detrainment process acting alone (i.e., there is no compensating entrainment) to decrease the area of the whole eddy of radius $R \sim 10^2$ km by half. From this time constant and from the variation of temperature/salinity on an isopycnal surface we could estimate the corresponding fluxes to the far-field (but the modification of the ring itself is obviously a more complicated question). The area change in Eq. (10) is $\frac{1}{2}(\pi R^2) \sim R^2$, so that

$$\Delta t \sim \frac{R}{U u_d}.$$

Since U is a typical velocity in the outer shear layer of the eddy, and since this is small compared to the maximum azimuthal velocity we shall take $U \sim 10$ cm s^{-1}. The remaining factor $u_d \sim 0.05$ [Eq. (9)] comes from our theory, and thus Eq. (11) yields

$$\Delta t \sim 1 \text{ year}.$$

Since the observed lifetime of a ring is of the order of a year, this calculation implies that a significant fraction of the isopycnal variation of temperature and salinity in the ring should be transferred to the far-field by the mechanism discussed here. Moreover the enhanced vertical gradients of temperature and salinity on the strained filament in that region should initiate the small-scale processes which lead to complete thermodynamic mixing.

REFERENCES

Ford, W. L., J. R. Longard and R. F. Banks, 1982: On the nature, occurrence, and origin of cold low-salinity water along the edge of the Gulf Stream. *J. Mar. Res.*, **11**, 281–293.

Pullin, D. I., 1981: The nonlinear behavior of a constant vorticity layer at a wall. *J. Fluid Mech.*, **108**, 401–421.

Ramp, S. R., 1986: The interaction of warm core rings with the shelf water and shelf/slope front south of New England. Ph.D. thesis, University of Rhode Island.

Stern, M. E., 1985: Lateral wave breaking and "shingle" formation in large-scale flow. *J. Phys. Oceanogr.*, **15**, 1274–1283.

——, 1986: On the amplification of convergences in coastal currents and the formation of "squirts". *J. Mar. Res.*, **44**, 403–421.

——, 1987: Horizontal entrainment and detrainment in large-scale eddies. *J. Phys. Oceanogr.*, **17**, 1688–1695.

Unauthenticated | Downloaded 12/02/23 06:42 AM UTC